AIAA 81-0489R

Finite Element Vibration Analysis of Damped Structures

M. L. Soni* and F. K. Bogner†
University of Dayton Research Institute, Dayton, Ohio

A finite element computer program, MAGNA-D, has been developed for predicting the response of damped structures to steady-state inputs. The use of a unique finite element library and efficient programming techniques make the procedure especially applicable to sizable three-dimensional structures composed of both solid and shell-like components. The program predicts frequencies and mode shapes, steady-state amplitudes and phase angles, and modal damping factors. The analysis includes the damping effects of viscoelastic materials characterized by complex moduli, and of Coulomb friction at sliding interfaces. Examples are presented to illustrate the utility and efficiency of the computer program.

Introduction

THE effectiveness of viscoelastic damping materials in forms such as free layer coatings or constrained layer treatments has been recognized for many years.[1-5] Until recently, layered damping concepts have been utilized primarily to resolve vibration problems in existing structures in an ad hoc manner; however, there is increasing activity in the development of general techniques for including the effects of various forms of damping at the initial design stage. The availability of accurate, efficient analysis tools is crucial to the design of reliable structures that include damping materials.

This paper describes a finite element computer program, MAGNA-D, which has been developed to analyze complex structures vibrating about nonlinear, prestressed configurations. The program predicts the amplitudes and phase angles of response quantities (displacements, strains, and stresses) that result from the application of steady-state force inputs. Particular emphasis has been focused on the solution of structures that are either three-dimensional or shell-like in nature. To this end, the program includes isoparametric thin shell and solid finite elements that are fully compatible, thus facilitating the analysis of sandwich and constrained layer construction. Damping analysis is performed by the complex stiffness (modulus and loss factor) approach (variation of material properties and damping factors with frequency is taken into account), and by consideration of the dissipation of vibratory energy through friction.

The following discussion includes a brief theoretical description of the problem considered, a summary of the distinguishing features of the MAGNA-D program, and the presentation of some typical applications.

Formulation

The present finite element formulation is based on the incremental virtual work principle of nonlinear elasticity. It is assumed that the configuration that the initially stressed vibrating structure attains is reached by a succession of two separate motions. First, the structure is subjected to the forces and constraints that are responsible for inducing the initial stresses and deformation. Second, the harmonic motion is superposed upon this initial deformed state. The harmonic motion is treated as linearly elastic. The formulation includes material and geometrical nonlinearities in the prestressed state. No further restrictions are made regarding the structural geometry and boundary conditions and the manner in which the initial state of stress is reached. A common initially stressed configuration is that which occurs as a result of rotation.

A summary of the derivation of the finite element equations that govern the forced vibrations of a model is presented below.

Consider a three-dimensional body in three different stages, as shown in Fig. 1. State C_0 is the undeformed, unstressed state of the body. State C_1 is an intermediate state of deformation, presumed to be known. This configuration represents the state of the body at the most recent state of load incrementation. State C_2 is the "final" state, to be determined upon application of an additional increment of loading. Actually, state C_2 is found by solving for the increment of deformation that occurs, and then adding the increment to the state C_1 deformation.

With a known intermediate or prestressed state C_1, the expression for incremental virtual work between states C_1 and C_2 is given by[7]

$$\int_{V_0} [D_{ijkl} e_{kl} \delta e_{ij} + {}_1\sigma_{ij} \delta \eta_{ij} + \rho_0 \ddot{u}_i \delta u_i] dV = \int_{V_0} f_i \delta u_i dV + \int_{\partial V_0} \bar{t}_i \delta u_i dA \tag{1}$$

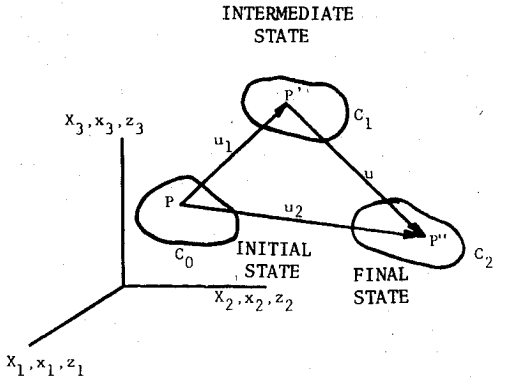

Fig. 1 Successive states of deformation of a three-dimensional body.

Presented as Paper 81-0489 at the AIAA/ASME/ASCE/AHS 22nd Structures, Structural Dynamics and Materials Conference, Atlanta, Ga., April 6-8, 1981; submitted April 15, 1981; revision received Sept. 24, 1981.

*Research Engineer, Analytical Mechanics Group.
†Group Leader, Analytical Mechanics Group. Member AIAA.

where the repeated indices indicate summation from 1 to 3, and

V_0 = volume in state C_0
∂V_0 = stress boundary in state C_0
ρ_0 = mass density in state C_0
${}_1\sigma_{ij}$ = stresses in state C_1
f_i = increments in applied body forces
t_i = increments in applied surface tractions
$D_{ijk\ell}$ = constitutive tensor relating increments of stress and increments of strain
u_i = increments in displacement from state C_1 to state C_2
$\ddot{u}_i$ = increments in acceleration
$e_{k\ell}$ = linear part of the increment in strain
η_{ij} = nonlinear part of the increment in strain
$\delta(\ )$ = virtual change

The first two terms on the left-hand side of the above equation represent the strain energy of incremental deformation and the work performed by the initial stress state during the incremental process, respectively. The third term accounts for the increment of work due to the inertial forces of acceleration. The incremental virtual work done by the prescribed increments in body forces and surface tractions appears on the right-hand side of the equation.

Following the usual finite element discretization procedure, the equations governing the time-dependent nonlinear response of the body are obtained as

$$(\underline{\underline{K}}+\underline{\underline{K}}_G)\underline{X}+\underline{\underline{M}}\ddot{\underline{X}}=\underline{F} \tag{2}$$

where a single underbar denotes a vector and a double underbar indicates a matrix.

As it stands, Eq. (2) forms the basis for the development of the MAGNA computer program described in Ref. 7. MAGNA is a large-scale program applicable to the static and transient dynamic analysis of complex three-dimensional structures experiencing large displacements, finite strains, large rotations, and plastic deformation. In this paper we consider a specialization of Eq. (2) that permits the development of an analysis method for predicting the linear, damped, steady-state response, of three-dimensional structures, about a nonlinear, initially stressed equilibrium configuration; this method is further specialized to permit the analysis of free vibrations in terms of natural frequencies and normal modes. In addition, Eq. (2) is modified to include the damping effects of friction at sliding interfaces.

Forced Vibrations with Hysteretic Damping

Consider that state C_1 of Fig. 1 is an equilibrium configuration which has been attained by a deformation (possibly nonlinear) from the original state C_0. Analytically, state C_1 is obtained by applying Eq. (1) as implemented in a computer program such as MAGNA-D.[6] In practice, a common form of state C_1 is that of a body rotating about a fixed axis. We consider here a modification of Eq. (2) that will permit the prediction of state C_2, the small forced oscillations of a body superposed on state C_1.

Consider the case when the applied forces (increments) in Eq. (2) are harmonic in time; that is,

$$\underline{F}=\tilde{\underline{F}}\,e^{i\omega t} \tag{3}$$

where ω is the forcing frequency, t is the time, and $i=\sqrt{-1}$. It is assumed that the response to the harmonic applied forces is also harmonic of the form

$$\underline{X}=\tilde{\underline{X}}e^{i\omega t} \tag{4}$$

where $\tilde{\underline{X}}$ is a vector of nodal displacements that characterize the spatial form of the response. The elements of $\tilde{\underline{X}}$ are, in general, complex owing to possible phase differences (due to damping) between the response quantities and the forcing function. Incorporation of Eqs. (3) and (4) into Eq. (2) leads to (after eliminating $e^{i\omega t}$ from each term)

$$[\tilde{\underline{\underline{K}}}+\underline{\underline{K}}_G-\omega^2\underline{\underline{M}}]\tilde{\underline{X}}=\tilde{\underline{F}} \tag{5}$$

This equation yields the small nodal vibrational response about a prestressed equilibrium state predicted by Eq. (2). The viscoelastic damping behavior is incorporated through the constitutive law

$$\underline{\sigma}=(\underline{\underline{D}}^R+i\underline{\underline{D}}^I)\,\underline{e} \tag{6}$$

where $\underline{\underline{D}}^R$ and $\underline{\underline{D}}^I$ are the matrices with frequency-dependent coefficients characterizing the energy storage and dissipative behavior of the material, respectively. The stiffness matrix $\tilde{\underline{\underline{K}}}$ is thus complex.

Vibrations with Coulomb Damping

An important consideration in the study of a class of problems such as turbine blades, is the determination of the effects of slip friction in reducing vibratory stresses. Other methods of reducing vibrations, such as the application of surface coatings, have not been extremely successful due, in part, to the high temperatures and rotation speeds that are common in modern turbines. Increasing the damping through the introduction of blade-to-disk and blade-to-blade interfaces has proved to be somewhat successful in controlling resonant response, due to the energy dissipated through friction contact when slip occurs at the interface.

In a recent study,[8] a small-order discrete spring/mass/damper/friction model has been used to model multiple interacting turbine blades. The results of this simplified analysis have been very encouraging. However, further refinements of the model using this approach present some difficult problems, such as the accurate estimation of appropriate numerical values for the springs, masses, and damping coefficients. A finite element modeling procedure of the slip-friction damping problem is developed herein.

The problem is formulated and solved in two steps:

1) The rotating equilibrium state is determined by solving a real-valued, undamped, nonlinear statics problem represented by

$$[\underline{\underline{K}}+\underline{\underline{K}}_G(\underline{X}_R)]\underline{X}_R=\underline{F}_R(\Omega^2) \tag{7}$$

which is obtained from Eq. (2) by setting the time derivatives to zero. In Eq. (7), $\underline{F}_R$ is the vector of node loads due to the rotation Ω, and $\underline{X}_R$ is the vector of node displacements due to the rotation. The $\underline{\underline{K}}_G$ matrix is retained to allow for the large deflections that may occur when a flexible structure like a fan blade uncurls because of high rotation speeds. In those cases, Eq. (7) is solved iteratively. For cases in which the structure is quite stiff, Eq. (7) can be solved as a linear static problem.

The solution to Eq. (7) is used to determine the internal forces acting at those nodes which will be subjected to slip-friction in step 2, and to include the centrifugal stiffening effects due to the rotation. In particular, the node forces normal to the sliding faces are determined; the computed surface normal force due to the rotation speed Ω at node k, for example, is denoted by $N_k(\Omega)$.

2) The equilibrium state determined from step 1 is subjected to harmonic forcing input, including the effects of viscoelastic damping (complex stiffness) and interface friction. The response is taken to be harmonic even under the influence of friction damping. Equation (2) is modified by including an additional term that accounts for the interface

friction; that is,

$$[\underline{\underline{K}}+\underline{\underline{K}}_G-\omega^2\underline{\underline{M}}]\underline{X}=\underline{F}-\underline{F}_F \tag{8}$$

where $\underline{F}_F$ is a vector containing the friction forces at the interface nodes, and zeros corresponding to other nodes. At a particular node k, the friction force is

$$f_k=\mu_k N_k(\Omega)\,(\dot{x}_k/|\dot{x}_k|) \tag{9}$$

where μ_k is the coefficient of friction, $N_k(\Omega)$ is the normal force computed in step 1, and $\dot{x}_k$ is the relative velocity at the interface tangent to the surface. The assumption has been made that the normal force $N_k(\Omega)$ is not altered significantly by the small vibration at this stage. The difference should be noted between the rotation speed Ω and the frequency ω of a "small" forcing function that induces steady-state oscillations about the rotating equilibrium configuration. It is also assumed, in addition to the harmonic force of Eq. (3) and the harmonic response given by Eq. (4), that x_k, the displacement tangent to the interface at node k, is also harmonic

$$x_k=X_k e^{i\omega t} \tag{10}$$

where X_k is complex. The nodal friction force of Eq. (9) then becomes

$$f_k=i\mu_k N_k(\Omega)\,(X_k/|X_k|) \tag{11}$$

Substitution of Eqs. (3), (4), and (11) into Eq. (8) and the admission again of complex moduli as material properties results in

$$[\underline{\underline{\tilde{K}}}+\underline{\underline{K}}_G-\omega^2\underline{\underline{M}}]\underline{\tilde{X}}=\underline{\tilde{F}}-\underline{\tilde{F}}_F \tag{12}$$

where $\underline{\tilde{F}}_F$ is a vector containing elements such as

$$\tilde{f}_k=i\mu_k N_k(\Omega)\,(X_k/|X_k|) \tag{13}$$

corresponding to those nodes on a friction interface, and zeros elsewhere.

Computer Program MAGNA-D

A computer program has been developed to implement the finite element equations above. The MAGNA-D[6] program is a large-scale, finite element system intended to analyze free vibrations and damped, steady-state, forced vibrations of complex structures. The program has been developed primarily for the efficient solution of structures composed of three-dimensional and shell-like components. Isoparametric modeling techniques and state-of-the-art solution techniques are combined in MAGNA-D to provide effective analytical capabilities. Both eigenvalue/eigenvector calculations (to compute natural frequencies and mode shapes), and simultaneous, complex equation solutions (to compute steady-state, forced response) are performed. Also, iterative solutions of nonlinear equations associated with the slip-friction phenomenon are considered. In addition, the program computes the modal damping factors of harmonically excited systems. The effects of frequency-dependent material properties are included. Convenience features such as incremental data generation, user subroutine interfaces, and pre- and postanalysis interactive graphics are included in MAGNA-D for more effective application to practical engineering problems. The program is presently operational on the CDC 6000 series and the CYBER 174 and 175 series mainframe computers, and on the VAX 11/780 minicomputer. Some of the salient features of the MAGNA-D program are summarized briefly below.

Finite Element Library

The finite element library of the MAGNA-D program currently contains three element types.

Three-Dimensional Solid with Variable Number of Nodes

This is an isoparametric element that can contain from 8 (trilinear, eight-node brick) to 27 nodes (triquadratic, 27-node brick). The element is shown in parametric space in Fig. 2. Two of the more common forms of this element are the 20-node brick used for modeling three-dimensional solids and the 16-node thick shell element. The order of numerical integration can be specified; for example, if reduced integration is used with the 20-node element, moderately thin shells can be modeled effectively.

Three-Dimensional Solid with Eight Nodes

This is the familiar eight-node brick obtained by considering only the corner nodes in Fig. 2. This element is programmed separately for reasons of efficiency. Because of the simple trilinear shape functions used in this element, it is used only where rather simple states of deformation are anticipated. A class of problems in which the eight-node brick performs well is layered sandwich construction. This element can be used effectively in modeling the sandwich core that is subjected primarily to transverse shear, using one-point integration.

Eight-Node Thin Shell Element

The use of the eight-node thin shell element[9,10] is a unique feature of the MAGNA and MAGNA-D programs. The geometry of the shell element is shown in Fig. 3. This is an eight-node isoparametric element similar in physical ap-

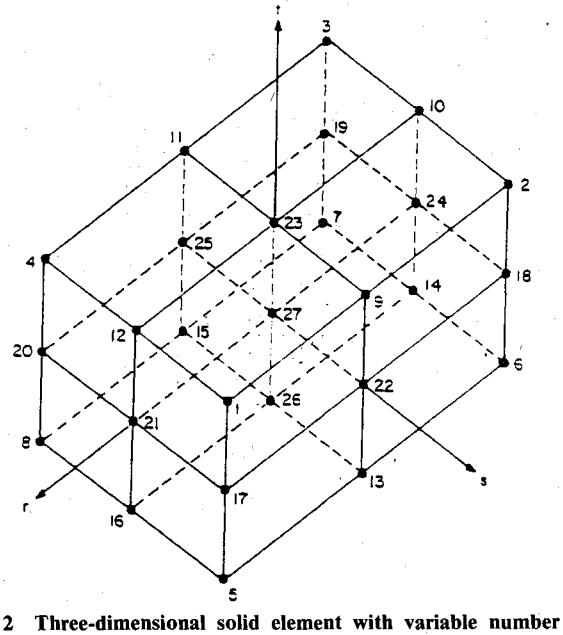

Fig. 2 Three-dimensional solid element with variable number of nodes.

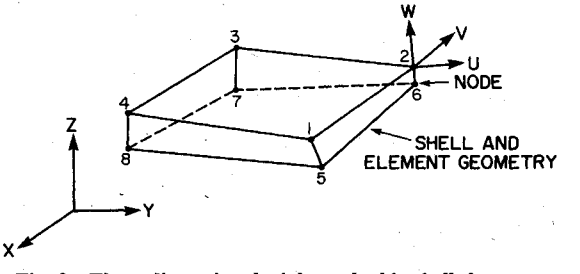

Fig. 3 Three-dimensional, eight-node thin shell element.

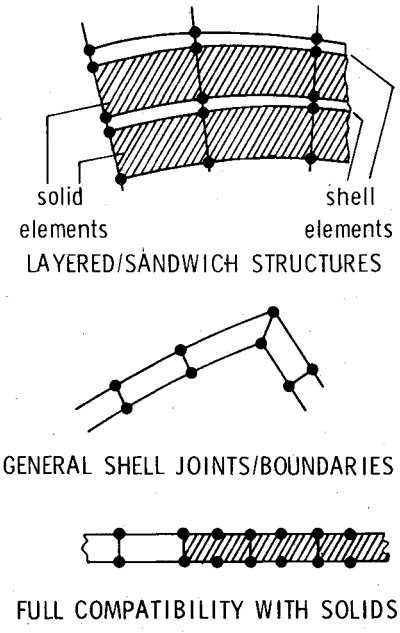

Fig. 4 Modeling capabilities of penalty function based shell element.

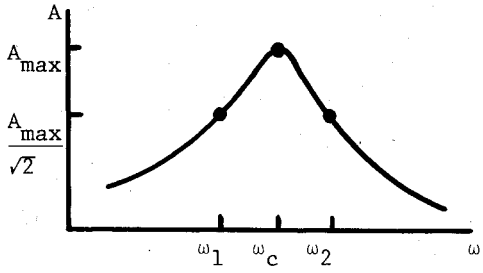

Fig. 5 Amplitude vs forcing frequency plot.

pearance to the eight-node brick element, as it has nodes only at the eight corners. Not only is this element similar in appearance to the eight-node brick, but it has the same number and types of degrees of freedom at the nodes—the three components of displacement. Therefore this particular shell element is fully compatible on all surfaces, with other penalty function shell elements and with conventional solid isoparametric elements. Therefore, layered shells, sandwich constructions, transitions between shells and solids, and joined shells are easily modeled with special constraints (Fig. 4).

The shell element can have variable thickness, and the lateral boundaries of the element need not be normal to the shell midsurface. The shell element is derived from three-dimensional elasticity theory by appending "penalty terms" which insure that the Love-Kirchoff hypothesis is satisfied for small thickness. By this approach to the element derivation, the necessity for inclusion of slope or rotation variables is avoided. The detailed development of this element is given in Refs. 9 and 10.

Forced Harmonic Analysis

Equation (5) represents a set of complex, linear algebraic equations. A solution to the equations for a particular value of the forcing frequency ω is obtained by the following steps:

Decomposition: $(\underline{\underline{\tilde{K}}} + \underline{\underline{K}}_G - \omega^2 \underline{\underline{M}}) = \underline{\underline{L}}\underline{\underline{D}}\underline{\underline{L}}^T$

Forward substitution: $\underline{\underline{L}}\underline{Z} = \underline{\tilde{F}}$

Scaling: $\underline{\underline{D}}\underline{Y} = \underline{Z}$

Back substitution: $\underline{\underline{L}}^T \underline{\tilde{X}} = \underline{Y}$

These operations have been programmed using out-of-core storage techniques so that large-scale systems of equations can be considered.

The above solution can be applied to Eq. (5) for a single forcing frequency, or, alternatively, a number of solutions can be obtained by sweeping through a number of specified frequencies. This capability is useful for making amplitude and phase angle vs frequency plots of displacements, strains, and stresses. System modal damping factors can be computed in two ways: by the half-power bandwidth method and by the strain energy ratio approach.

Figure 5 shows a portion of typical amplitude vs forcing frequency plot for forcing frequencies in the vicinity of a resonance. The half-power bandwidth computation of the modal damping factor η_{si} for the ith mode is made by evaluating

$$\eta_{si} = (\omega_2 - \omega_1)/\omega_c \tag{14}$$

where ω_c is the frequency corresponding to the maximum amplitude, and ω_1 and ω_2 are the frequencies associated with amplitudes $A_{\max}/\sqrt{2}$.

The energy ratio approach to the computation of modal damping factors is expressed as

$$\eta_{si} = \sum_{j=1}^{N} \eta_j W_{jc}^{(i)} \Big/ \sum_{j=1}^{N} W_{jc}^{(i)} \tag{15}$$

where N is the number of finite elements in the model, η_j is the material damping factor (defined as $\underline{\underline{D}}^I = \eta \underline{\underline{D}}^R$) for element j, and $W_{jc}^{(i)}$ is the energy stored in the jth element when the system is being forced at frequency ω_c (Fig. 5).

Forced Harmonic Analysis with Coulomb Friction

The first step of the two-stage process for analyzing rotating systems with slip friction damping is to solve Eq. (7). For relatively flexible structures, the second term involving the geometric stiffness matrix is significant and the problem is a nonlinear one. In those cases, Eq. (7) is solved iteratively. For cases in which the structure is quite stiff, one pass through the iterative loop suffices.

The second step is to solve Eq. (12) for the forced vibrations of the system about the equilibrium state computed in step 1. This equation is nonlinear by virtue of the friction force term whose elements have the form given by Eq. (13). The solution process is an iterative one, with the first iteration being computed from a linear problem obtained by setting $\underline{\tilde{F}}_F = 0$. Further iterations are obtained by making successive evaluations of the linear equation

$$[\underline{\underline{\tilde{K}}} + \underline{\underline{K}}_G - \omega^2 \underline{\underline{M}}]\underline{\tilde{X}}^{(i+1)} = \underline{\tilde{F}} - \underline{\tilde{F}}_F^{(i)} \tag{16}$$

Solutions can be obtained by imposing a single forcing frequency, or frequency sweeps can be performed in which a range of forcing frequencies is specified. Equivalent modal damping factors are calculated using either Eq. (14) or (15).

Demonstration Problems

The MAGNA-D program described above has been used to solve many numerical examples. The results of a few of these examples are presented below.

Sandwich Cantilever Beam

The first case considered is that of a sandwich cantilever beam[11] with constrained layer damping treatment. This problem has been studied extensively in various analyses and experiments.[12] The effect of shearing capability of the

viscoelastic layer upon the damped frequency and loss-factor of the composite beam was first analyzed for infinite length beams in Ref. 13 using an effective stiffness method and the classical fourth-order theory of elastic beams. In Ref. 1 energy approach was introduced to define the beam loss-factor. For finite length beams a sixth-order theory was derived and solved for various boundary conditions in Refs. 14-16. The problem has also been analyzed using various finite-element programs.[17,18] More recently, the sandwich beam has been used in damping characterization of polymeric materials.[19]

The geometry of the beam shown in Fig. 6 and the properties given in Table 1 are those used in an actual test specimen.[19] Two different cases of damping layer materials are considered. In the first, the damping layer is taken to be 3M-ISD468 adhesive with the frequency- and temperature-dependent material properties found in Ref. 19; in the second case, a hypothetical damping material with frequency-invariant material properties is used.[18]

The base and the constraining layers are discretized using the eight-node thin shell elements, and the solid elements with eight corner nodes and reduced integration are used to model the damping layer; each layer employed 22 elements of respective type. A total of 184 nodes with 440 active degrees of freedom are used in the model. Damped forced response is obtained using the complex stiffness method for the first six flexural modes of vibrations.

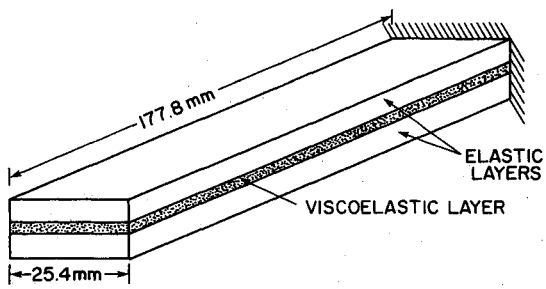

Fig. 6 Cantilevered beam with constrained layer damping treatment.

Table 1 Material properties of sandwich beam

	Elastic layer	Viscoelastic layer
Thickness, mm	1.524	0.127
Young's modulus, N/m^2	6.9×10^{10}	[a] 2.1×10^{6}
Poisson's ratio	0.3	0.499
Damping factor		[a] 0.1, 0.3, 1, 1.5
Density, kg/m^3	2.8×10^{4}	9.7×10^{2}

[a] 3M-ISD468 damping material with frequency dependent properties.

Table 2 Modal properties cantilevered beam with constrained layer damping

Mode	Frequency, Hz FEA[a]	Frequency, Hz Experiment[19]	Modal loss factor FEA	Modal loss factor Experiment
1	82	...	.0049	...
2	505	510	.0101	.006
3	1394	1402	.0123	.009
4	2690	2699	.0148	.014
5	4375	4380	.017	.018

[a] Present finite element analysis.

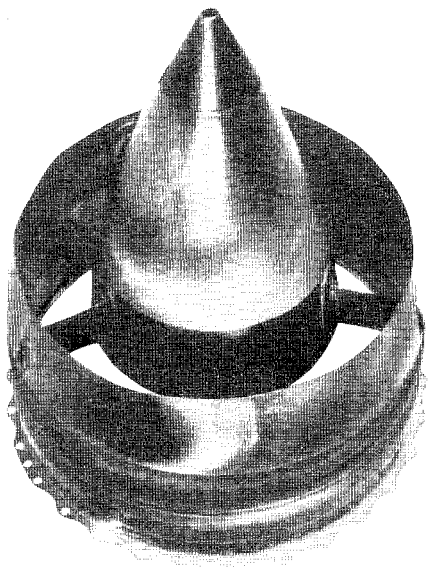

Fig. 7 Jet engine exhaust duct.

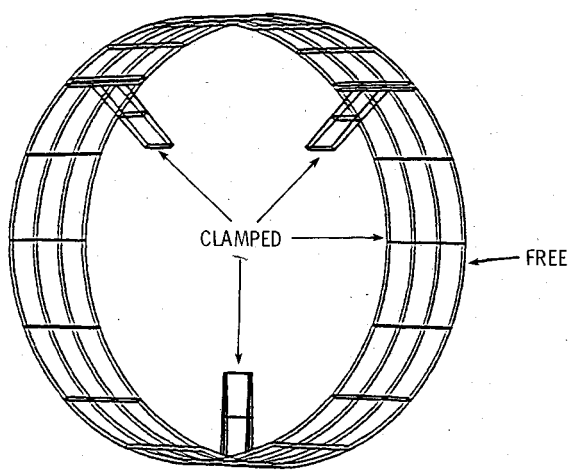

Fig. 8 Finite element model of engine exhaust duct.

Table 3 Core loss factor and modal properties of cantilevered beam with constrained layer damping

Core loss factor	Method of analysis	Mode 1 ω[c]	Mode 1 $\bar{\eta}$[d]	Mode 2 ω	Mode 2 $\bar{\eta}$	Mode 3 ω	Mode 3 $\bar{\eta}$	Mode 4 ω	Mode 4 $\bar{\eta}$	Mode 5 ω	Mode 5 $\bar{\eta}$	Mode 6 ω	Mode 6 $\bar{\eta}$
0.1	a	64.075	0.2815	296.41	0.2424	743.7	0.154	1393.9	0.0889	2261.09	0.0573	3343.6	0.0390
	b	64.2	0.2817	297.	0.2425	747.2	0.1534	1408.3	0.0878	2304.	0.0559	3446.1	0.0377
	a	64.43	0.2723	297.01	0.2399	744.1	0.1538	1394.	0.0888	2261.24	0.0572	3343.7	0.039
0.3	b	64.7	0.2725	298.	0.2401	748.2	0.1531	1409.5	0.0878	2305.	0.056	3447.	0.0372
	a	67.41	0.2022	302.8	0.2177	748.6	0.1502	1396.6	0.0881	2262.88	0.0570	3345.	0.0389
1.0	b	67.4	0.2019	307.	0.218	762.	0.15	1422.	0.0873	2316.	0.056	3455.	0.0377
	a	69.88	0.1531	308.85	0.1975	754.	0.146	1399.7	0.0873	2265.	0.0568	3346.	0.0389
1.5	b	70.	0.1522	315.	0.1952	774.	0.1457	1433.	0.0868	2328.	0.0559	3468.5	0.0378

[a] Sixth-order theory of Refs. 16 and 18. [b] Present finite element analysis. [c] ω = damped resonance frequency in Hertz. [d] $\bar{\eta}$ = loss factor parameter (= modal loss factor/core loss factor).

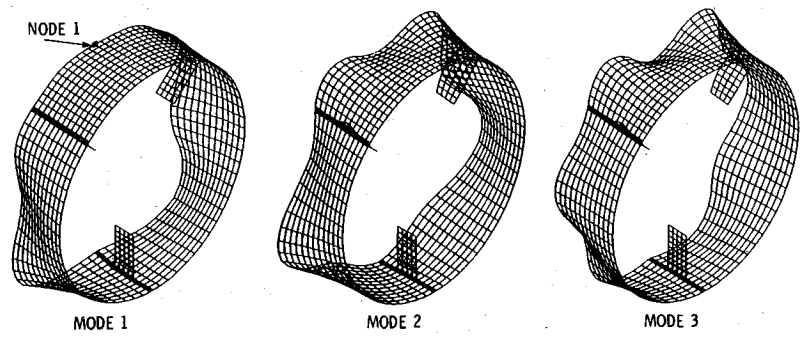

Fig. 9 Mode shapes of engine exhaust duct (perspective view).

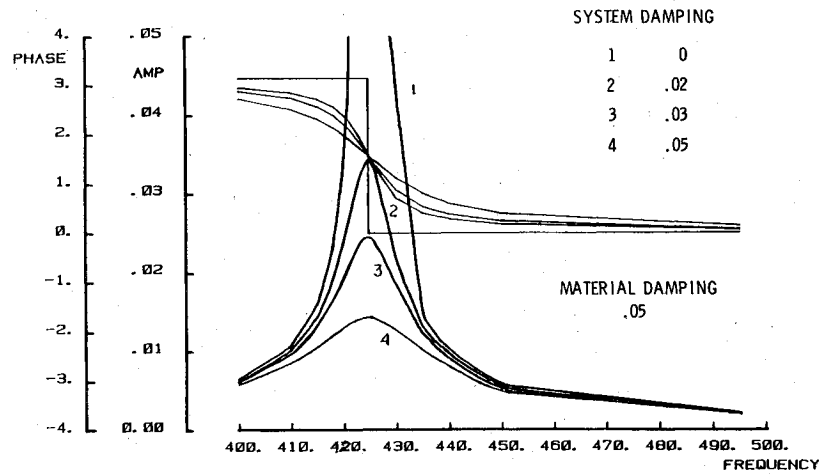

Fig. 10 Engine exhaust duct, effect of damping treatment on the amplitude frequency response of second mode of forced vibrations: 1) no damping, 2) vanes only, 3) shroud only, 4) shroud and vanes.

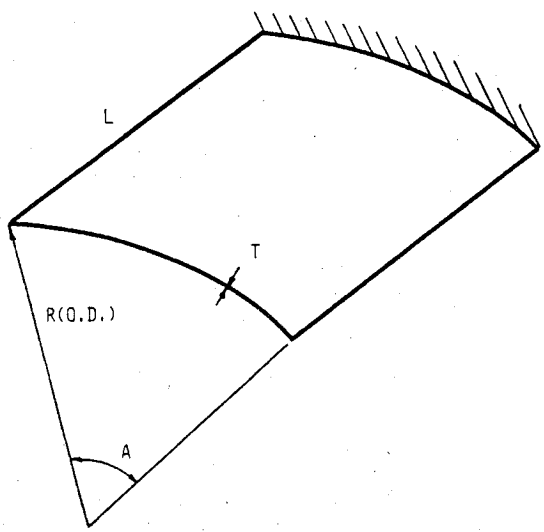

Fig. 11 Clamped cylindrical panel, $L = 305$ mm, $R = 610$ mm, $T = 1.6$ mm, $A = 30$ deg.

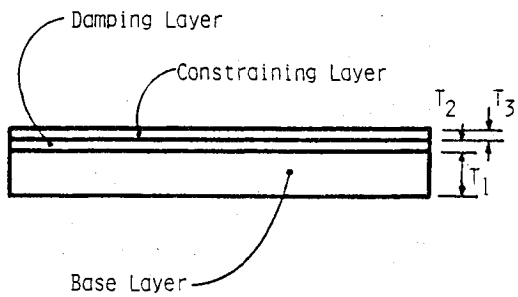

Fig. 12 Layer geometry of panel with damping treatment.

The damped frequencies and corresponding modal loss factors obtained from the finite-element analysis are compared to those of laboratory experiment in Table 2. The damping material with frequency-dependent properties is taken for this case.

The values of damped resonance frequencies are in excellent agreement, and the modal loss factor also compares well, except at very low damping. This discrepancy may be attributed to the errors in the measurement. At very small damping, the sharpness of the amplitude-frequency response curve makes it difficult to locate the half-power bandwidth points. For further comparisons, the beam problem with frequency-independent material properties is solved for various values of core loss factor. The results are presented in Table 3, where the corresponding results of sixth-order theory[16,18] are also shown. The two analyses are in excellent agreement for the range of frequencies and core loss factors considered.

Damping Analysis of Jet Engine Exhaust Duct

This demonstration problem is similar to the jet engine exhaust duct shown in Fig. 7. Not having a complex description of the geometry and properties of the exhaust duct, a hypothetical structure having the basic physical characteristics is modeled for the purpose of illustration. The finite element model considered is shown in Fig. 8.

A cylindrical shroud with three flat vanes has been modeled with a variable number of node solid elements. Although the full structure is shown, only a symmetric half of the structure on one side of a plane of symmetry through the bottom vane has been modeled for computation. The boundary conditions are indicated on the figure. The dimensions and material of the shroud and vanes are as follows: shroud—254 mm i.d., 1.27 mm thick, 76.2 mm wide, steel; vanes—63.5 mm long, 2.54 mm thick, 25.4 mm wide, steel.

A natural vibration analysis of the model of Fig. 8 has been performed with the MAGNA-D program. Perspective plots of the first three mode shapes are shown in Fig. 9.

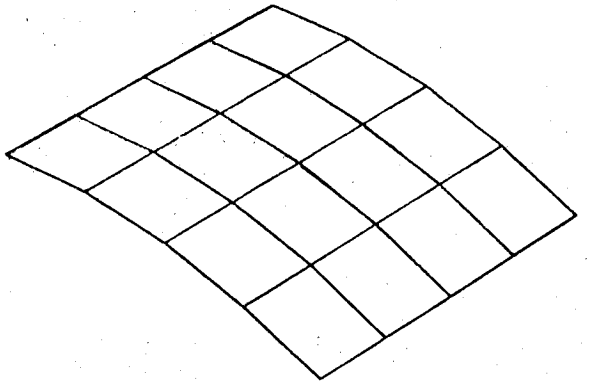

Fig. 13 Finite element model of layered panel.

In practice, a damping treatment might be applied to one or more exposed surfaces of the structure. In order to keep the model relatively small for illustration purposes, we assume that the shroud and/or the vane material is internally damped. This assumption permits a one-layer model to be considered (multiple layers could be considered, however). Four different cases are treated: 1) no damping, 2) vane elements with 5% damping, 3) shroud elements with 5% damping, and 4) shroud and vane elements with 5% damping. For each of the cases, Eq. (5) has been solved for several forcing frequencies on either side of the first undamped natural frequency. The forcing excitation is a harmonically varying concentrated normal force applied to the node at the top of the free edge of the shroud in Fig. 8. The solution to Eq. (5) provides amplitudes and phase angles for every node in the structure. For the node at which the force is applied, the amplitude and phase angle vs forcing frequency plot is shown in Fig. 10 for the above four cases.

The finite element model for this program resulted in 414 independent degrees of freedom. It should be noted that these are complex degrees of freedom (involving both amplitude and phase angle), which are determined by solving Eq. (5). To generate the results in Fig. 10, a frequency sweep over 20 forcing frequencies was used for each of the four cases. Each curve required 66 s of CDC CYBER 175 central processing time. Therefore 80 separate solutions to Eq. (5) required a total of only 264 s.

Cylindrical Panel with Constrained Layer Damping

Consider the hypothetical aluminum cylindrical panel shown in Fig. 11. The panel is coated with a layer of viscoelastic damping material and a constraining layer, as indicated in Fig. 12. Table 4 contains the properties of the various layers. A finite element model of the structure is shown in Fig. 13. The base and constraining layer are modeled with penalty function shell elements, and the damping layer is modeled with eight-node solid brick elements. The constraining layer and the damping layer cannot be detected in Fig. 13, since they are thin as compared with the base layer.

A concentrated harmonic force at one of the corners of the panel was used to excite the system. A frequency sweep was performed over a range of forcing frequencies, and for each of the several values of material damping factor η_m indicated in Table 4. The amplitude of the displacement under the load vs the forcing frequency is shown in Fig. 13 for the various material loss factors. The decrease in maximum amplitude as η_m increases is apparent in Fig. 14. Figure 15 shows the variation of the maximum amplitude of the second mode vs the material damping factor.

Conclusions

The equations which govern the steady-state, forced, damped vibrations of complex structures have been formulated. The solution to the derived equations has been implemented into a comprehensive finite-element computer program, MAGNA-D. Particular attention has been focused in the program on the efficient solution of three-dimensional and shell structures. Analysis capabilities include natural frequency and normal mode anlaysis, forced harmonic analysis with and without slip-friction, and modal damping analysis using the modal strain energy approach. Three examples have been presented to demonstrate the applicability of the MAGNA-D program to the solution of problems of practical interest.

Table 4 Layer properties of sandwich cylindrical panel

	Base layer	Damping layer	Constraining layer
Young's modulus, N/m^2	6.9×10^{10}	2.1×10^{6}	6.9×10^{10}
Shear modulus, N/m^2		6.9×10^{5}	
Poisson's ratio	0.3		0.3
Thickness, mm	1.6	0.127	0.127
Damping factor	0	0.05 0.10 0.50 1.0 2.0	0
Density, kg/m^3	2.8×10^{4}	9.7×10^{2}	2.8×10^{4}

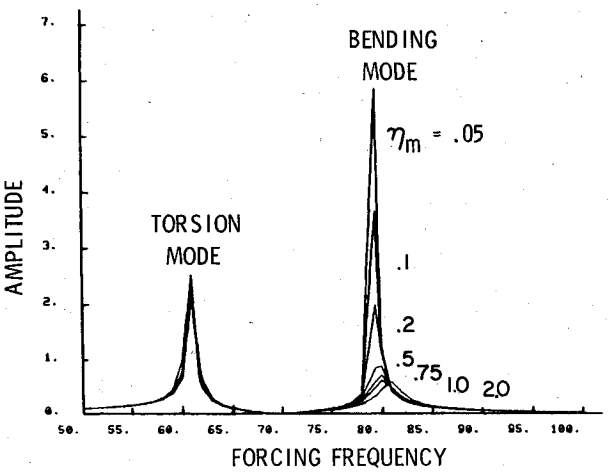

Fig. 14 Peak amplitude vs forcing frequency response.

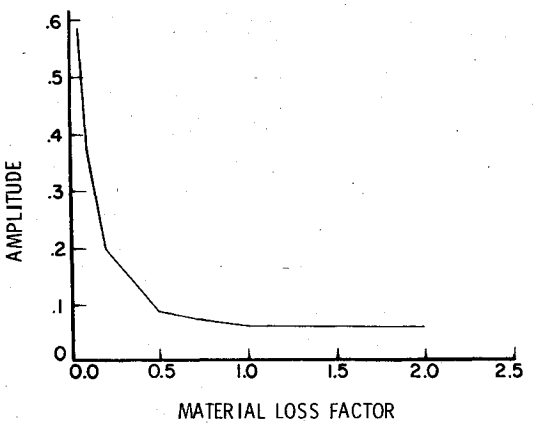

Fig. 15 Peak amplitude vs loss factor of the damping layer.

Acknowledgments

This work was supported in part by the Air Force Materials Laboratory and the Air Force Flight Dynamics Laboratory.

References

[1]Ungar, E., "Loss-Factors of Viscoelastically Damped Beam Structures," *Journal of the Acoustical Society*, Vol. 34, Aug. 1962, pp. 1082-1089.

[2]Oberst, H., "Reduction of Noise by the Use of Damping Materials," *Royal Aeronautical Society*, Vol. 263, 1968, pp. 411-453.

[3]Jones, D.I.G. and Cannon, C. M., "Control of Gas Turbine Stator Blade Vibrations by Means of Enamel Coatings," *Journal of Aircraft*, Vol. 12, April 1975, pp. 226-230.

[4]Henderson, J. P., "Investigation of the Effect of Damping Treatment on the Response of Heated Fuselage Structure," Vibration Damping Short Course, University of Dayton Research Institute, Oct. 1978.

[5]Rogers, L. C. and Parin, M. L., "A Thoroughly Engineered Application of Damping Technology to Jet Engine Inlet Guide Vanes," Conference on Aerospace Polymeric Viscoelastic Damping Technology for the 1980's, AFFDL-TM-78-FBA, July 1978.

[6]Soni, M. L., "Finite Element Analysis of Vibrations of Initially Stressed Viscoelastic Structures," University of Dayton Tech. Rept. UDR-TR-79-113, Nov. 1979.

[7]Brockman, R. A., "MAGNA Computer Program User's Manual," University of Dayton Rept. UDR-TR-80-107, Nov. 1980; see also AFWAL-TR-80-3152, Jan. 1981.

[8]Muszynska, A. and Jones, D.I.G., "On Discrete Modellization of Response of Blades with Slip and Hysteretic Damping," *Proceedings of the Fifth World Congress on Theory of Machines and Mechanisms*, ASME, New York, 1979, pp. 646-649.

[9]Brockman, R. A., "A Penalty Function Approach for the Nonlinear Finite Element Analysis of Thin Shells," Ph.D. Thesis, University of Dayton, Dayton, Ohio, July 1979.

[10]Brockman, R. A. and Bogner, F. K., "An Efficient Three-Dimensional Shell Finite Element for Highly Nonlinear Problems," paper presented at the ASME Century 2 International Computer Technology Conference, San Francisco, Calif., Aug. 1980.

[11]Soni, M. L., "Finite Element Analysis of Viscoelastically Damped Sandwich Structures," *The Shock and Vibration Bulletin*, Vol. 51, Pt. 1, May 1981, pp. 97-109.

[12]Nakra, B. C., "Vibration Control with Viscoelastic Materials," *The Shock and Vibration Digest*, Vol. 8, June 1975, pp. 114-123.

[13]Kerwin, E. M., "Damping of Flexural Waves by a Constrained Viscoelastic Layer," *The Journal of the Acoustical Society of America*, Vol. 32, July 1959, pp. 952-962.

[14]Ditaranto, R. A., "Theory of Vibratory Bending for Elastic and Viscoelastic Layered Finite Length Beams," *Journal of Applied Mechanics*, Vol. 32; *Transactions of the ASME, Series E*, Vol. 87, Dec. 1965, pp. 881-886.

[15]Mead, D. J. and Markus, S., "Loss-Factors and Resonant Frequencies of Encastré Damped Sandwich Beams," *Journal of Sound and Vibration*, Vol. 12, Jan. 1970, pp. 99-112.

[16]Rao, D. K., "Frequency and Loss Factors of Sandwich Beams Under Various Boundary Conditions," *Journal of Mechanical Engineering Science*, Vol. 20, May 1978, pp. 271-282.

[17]Carne, T., "Constrained Layer Damping Examined by Finite Element Analysis," *Proceedings of the Society of Engineering Science, 12th Annual Meeting*, Austin, Texas, Oct. 1975, pp. 567-576.

[18]Rogers, L. C., Johnson, C. D., and Keinholtz, D. A., "The Modal Strain Energy Finite Element Analysis Method and its Application to Damped Laminated Beams," paper presented at the 51st Shock and Vibration Symposium, San Diego, Calif., Oct. 1980.

[19]Drake, M. L. and Turborg, G. E., "Polymeric Materials Testing Procedures to Determine the Damping Properties and the Result of Selected Commercial Materials," University of Dayton Tech. Rept. UDR-TR-80-40, 1980.